MOX-Report No. 83/2022

Unmapped tent pitching schemes by waveform relaxation

Ciaramella, G.; Gander, M.; Mazzieri, I.

Unmapped tent pitching schemes by waveform relaxation

Gabriele Ciaramella, Martin J. Gander and Ilario Mazzieri

1 Introduction

The *mapped tent pitching* algorithm (MTP) is a very advanced domain decomposition strategy for the parallel solution of hyperbolic problems. MTP was introduced in [4] and computes the solution by iteratively constructing new polygonal space-time subdomains, called *tents*, in a way that the hyperbolic problem can be solved exactly within them. Due to the polygonal space-time structure of the subdomains, the numerical solution is obtained by a process that maps the tents into space-time cylinders (rectangles for 1D spatial problems), computes the solution in the transformed subdomains, and maps it back into the original tents. Due to the tent mapping leading to singularities, special time integrators are needed to mitigate order reduction.

To avoid this, we introduce a new, *unmapped tent pitching* algorithm (UTP), based on a conceptual idea from Nievergelt in 1964 [5]: "In numerical analysis, one has always tried to speed up computation by reducing the amount of work to be done, not by performing redundant computations." Introducing redundant computations, we eliminate the mapping process from the MTP with a Schwarz waveform relaxation method (SWR). We present our new UTP for the model problem

$$
\begin{aligned}
\partial_{tt} u(x,t) = c^2 \partial_{xx} u(x,t) \ \text{ for } (x,t) \in \Omega \times (0,T), \\
u(x,0) = g_0(x) \text{ and } \partial_t u(x,0) = g_1(x) \ \text{ for } x \in \Omega, \\
u(0,t) = u(1,t) = 0 \ \text{ for } t \in [0,T],
\end{aligned}
\tag{1}
$$

G. Ciaramella
Politecnico di Milano, Italy, e-mail: gabriele.ciaramella@polimi.it

M.J. Gander
Université de Génève, Switzerland, e-mail: martin.gander@unige.ch

I. Mazzieri
Politecnico di Milano, Italy, e-mail: ilario.mazzieri@polimi.it

where $\Omega = (0,1)$, $T > 0$, and g_0 and g_1 are sufficiently regular functions. We first explain in Section 2 the classical MTP process for the solution of (1) and characterize the corresponding advancing front in case of a uniform space decomposition. Then, in Section 3, we introduce a red-black Schwarz waveform relaxation method (RBSWR) and prove a particular relation between RBSWR and MTP. This relation leads us very naturally to introduce our UTP in Section 4.

2 The mapped tent-pitching algorithm (MTP)

To describe the MTP algorithm introduced in [4] for the solution of (1), consider a set $\Omega_0 = \{x_j\}_{j=0}^N \subset \Omega$ of nodes $0 = x_0 < x_1 < \cdots < x_N = 1$. The core of MTP is the strategy used to *pitch tents* at the nodes and define the *advancing front* of the computed exact solution. In our one-dimensional setting, a tent is a hat-function ϕ_j with value 1 at the node x_j and zero at the remaining nodes of Ω_0. The advancing front (at iteration $k \in \mathbb{N}$) is a continuous functions $\tau_k^{\mathrm{MTP}} : \Omega \to \mathbb{R}$, which is linear in the subintervals (x_j, x_{j+1}). The MTP iteration is initialized with $\tau_0^{\mathrm{MTP}} \equiv 0$ and at the k-th iteration a new advancing front τ_k^{MTP} is computed from $\tau_{k-1}^{\mathrm{MTP}}$ with the property that $\tau_k^{\mathrm{MTP}}(x) \geq \tau_{k-1}^{\mathrm{MTP}}(x)$ for all $x \in \Omega$. The process terminates when an iteration $k = K > 0$ is reached with $\tau_K^{\mathrm{MTP}} \equiv T$. To obtain τ_k^{MTP} one needs to *pitch a new tent* on the front $\tau_{k-1}^{\mathrm{MTP}}$, that means to select an appropriate node x_j in Ω_0 and a $v_j^k > 0$, and update the advancing front as

$$\tau_k^{\mathrm{MTP}}(x) := \tau_{k-1}^{\mathrm{MTP}}(x) + v_j^k \phi_j(x). \tag{2}$$

The node x_j and the value v_j^k are computed to ensure that $|(\tau_k^{\mathrm{MTP}})'(x)| \leq \frac{1}{c}$ for all $x \in \Omega \setminus \Omega_0$. This is a CFL condition [2] and since τ_k^{MTP} is piecewise linear, it is equivalent to[1]

$$\frac{|\tau_k^{\mathrm{MTP}}(x_\ell) - \tau_k^{\mathrm{MTP}}(x_{\widetilde{\ell}})|}{|x_\ell - x_{\widetilde{\ell}}|} \leq \frac{1}{c} \ \text{ for all } \ell = 0, \ldots, N \text{ and } \widetilde{\ell} \in \mathcal{N}_\ell, \tag{3}$$

where $\mathcal{N}_\ell$ denotes the set of indices of the neighboring nodes to x_ℓ. Now, since ϕ_j is zero on $\Omega_0 \setminus \{x_j\}$, one has that $\tau_k^{\mathrm{MTP}}(x_\ell) = \tau_{k-1}^{\mathrm{MTP}}(x_\ell)$ for all $x_\ell \in \Omega_0 \setminus \{x_j\}$. Thus, given a $\tau_{k-1}^{\mathrm{MTP}}$ satisfying (3), the new tent must be pitched in a way that τ_k^{MTP} satisfies (3) as well, that is

$$\frac{|\tau_{k-1}^{\mathrm{MTP}}(x_j) + v_j^k \phi_j(x_j) - \tau_{k-1}^{\mathrm{MTP}}(x_{\widetilde{\ell}})|}{|x_j - x_{\widetilde{\ell}}|} \leq \frac{1}{c} \ \text{ for all } \widetilde{\ell} \in \mathcal{N}_j. \tag{4}$$

---

[1] In [4], condition (3) appears with an additional constant depending on the shape regularity of the decomposition. This constant is 1 in our one-dimensional framework.

Algorithm 1 Mapped Tent Pitching (sequential)

Require: A decomposition Ω_0.

1: Set $k = 0$ and initialize $\tau_k^{\mathrm{MTP}} \equiv 0$.

2: **while** $\tau_k^{\mathrm{MTP}} \not\equiv T$ **do**

3:     Compute the set J_k.

4:     Select an index $j \in J_k$, the corresponding node x_j and set $v_j^k = w_j^k$.

5:     Update the advancing front: $\tau_k^{\mathrm{MTP}}(x) := \tau_{k-1}^{\mathrm{MTP}}(x) + v_j^k \phi_j(x)$.

6:     Solve (1) in the domain between τ_k^{MTP} and $\tau_{k-1}^{\mathrm{MTP}}$ (below the new tent).

7:     Update $k = k + 1$.

8: **end while**

Since $v_j^k \phi_j(x) \geq 0$, $\tau_{k-1}^{\mathrm{MTP}}$ satisfies (3), and $\phi_j(x_j) = 1$, (4) becomes $v_j^k \leq \min_{\widetilde{\ell} \in \mathcal{N}_j} \left(\frac{|x_j - x_{\widetilde{\ell}}|}{c} + \tau_{k-1}^{\mathrm{MTP}}(x_{\widetilde{\ell}}) - \tau_{k-1}^{\mathrm{MTP}}(x_j) \right)$. To satisfy this condition and maximize the advancement of the front, we define

$$w_\ell^k := \min\left(T - \tau_{k-1}^{\mathrm{MTP}}(x_\ell), \min_{\widetilde{\ell} \in \mathcal{N}_\ell} \left(\frac{|x_\ell - x_{\widetilde{\ell}}|}{c} + \tau_{k-1}^{\mathrm{MTP}}(x_{\widetilde{\ell}}) - \tau_{k-1}^{\mathrm{MTP}}(x_\ell) \right) \right) \quad (5)$$

for $\ell = 1, \ldots, N$, and the set of admissible values v_j^k as $J_k := \{\ell \in \{1, \ldots, N\} : w_\ell^k > 0\}$. Thus, at the k-th iteration MTP selects any node x_j with $j \in J_k$ and pitches a tent of height $v_j^k = w_j^k$. Once a new tent is pitched, MTP solves the problem within this new tent by a mapping process that transforms the tent into a cylinder (a rectangle in this one-dimensional setting). The overall MTP procedure is given in Algorithm 1. This is the sequential version of MTP. A parallel version can be easily obtained by pitching multiple tents at each iteration, namely by modifying Step 4 and Step 5:

4: Select a set $\mathcal{S}_k \subset J_k$ of all indices $j \in \mathcal{S}_k$ such that the corresponding nodes are not neighbors. Pick all nodes x_j with $j \in \mathcal{S}_k$ and set $v_j^k = w_j^k$.

5: Update the advancing front: $\tau_k^{\mathrm{MTP}}(x) := \tau_{k-1}^{\mathrm{MTP}}(x) + \sum_{j \in \mathcal{S}_k} v_j^k \phi_j(x)$.

We illustrate the parallel MTP procedure with an example using a space decomposition of 7 points (x_j, $j = 0, \ldots, 6$), see Fig. 1, top left. The MTP is initialized with $\tau_0^{\mathrm{MTP}} \equiv 0$. For $k = 1$ all nodes can be potentially selected, that is $J_1 = \{0, \ldots, 6\}$, but not all of them can be simultaneously selected. Thus, we assume that the nodes x_1, x_3 and x_5 are selected and three tents are pitched on τ_0^{MTP}. The new resulting front is τ_1^{MTP}, which is represented by the red line in Fig. 1, top left. Notice that the slopes of τ_1^{MTP} are lower or equal to the slopes of the characteristic curves, because of condition (5) and the fact that the decomposition considered is nonuniform[2]. Once τ_1^{MTP} is obtained, the set of admissible nodes is $J_2 = \{0, 2, 4, 6\}$. These can be all selected and give rise to the hat-functions (multiplied by the corresponding values v_j^k) represented by the blue dashed lines in Fig. 1, top right. The new front τ_2^{MTP} (blue line in Fig. 1, top right) is then obtained by summing all

---

[2] For uniform decompositions, tents are always pitched along characteristic lines.
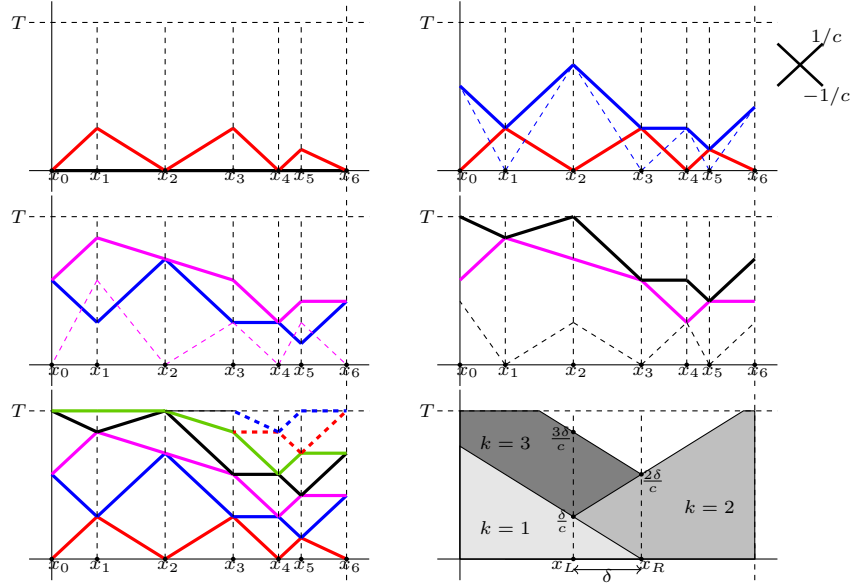
Fig. 1 Top row, left: MTP iteration 1: τ_1^{MTP} (red) and τ_0^{MTP} (black). The tents $v_j^1 \phi_j$ coincide with the red lines. The cross on the top right gives the slopes of the characteristic lines. **Top row, right**: MTP iteration 2: τ_2^{MTP} (blue), τ_1^{MTP} (red), new tents $v_j^2 \phi_j$ (blue dashed). **Middle row, left**: MTP iteration 3: τ_3^{MTP} (magenta), τ_2^{MTP} (blue), new tents $v_j^3 \phi_j$ (magenta dashed). **Middle row, right**: MTP iteration 4: τ_4^{MTP} (black), τ_3^{MTP} (magenta), new tents $v_j^4 \phi_j$ (black dashed). **Bottom row, left**: Full decomposition constructed by MTP. **Bottom row, right**: First three iterations of SWR. The gray areas are the regions where the exact solution is computed.

these functions to τ_1^{MTP}. Repeating this process at iterations 3 and 4 leads to the fronts τ_3^{MTP} (magenta line in Fig. 1, middle left) and τ_4^{MTP} (black line in Fig. 1, middle right). At convergence, we obtain the decomposition shown in Fig. 1, bottom left, which is not uniform since the initial space decomposition Ω_0 is not uniform. It is finer (in time) where the space decomposition is finer, and the front advances more slowly there. Note also that at each iteration the MTP process solves the problem below characteristics, and the conditions used to pitch new tents are satisfied when exact data is available on the lower boundary of the new tent and can be propagated into it. We now characterize the behavior of the advancing front for a uniform decomposition.

Lemma 1 (MTP advancing front for uniform decompositions)

Let the decomposition Ω_0 be uniform with $h := x_j - x_{j-1}$ for $j = 1, \ldots, N$. Consider any interior subinterval $\mathcal{I} = [x_L, x_R]$, with $R \in \mathbb{N}$ even and $L = R - 1$. Assume that the (parallel) MTP selects alternatingly odd and even nodes of Ω_0 at odd and even iterates, respectively. Then, starting from $\tau_0^{\mathrm{MTP}} \equiv 0$, we have that $\tau_1^{\mathrm{MTP}}(x_L) = \frac{h}{c}$ and $\tau_1^{\mathrm{MTP}}(x_R) = 0$, and for any $n > 0$ that

$$\tau_{2n}^{\mathrm{MTP}}(x_L) = (2n-1)h/c \qquad\qquad \tau_{2n}^{\mathrm{MTP}}(x_R) = 2nh/c, \qquad (6a)$$

$$\tau_{2n+1}^{\mathrm{MTP}}(x_L) = (2n+1)h/c, \qquad\qquad \tau_{2n+1}^{\mathrm{MTP}}(x_R) = 2nh/c. \qquad (6b)$$

Proof Denote by $\mathcal{N}_\ell$ the set of neighboring nodes of x_ℓ. The proof works by induction and uses (2) and (5). We begin with the base case $n = 0$. Since $\tau_0^{\mathrm{MTP}} \equiv 0$, using (5) we compute $v_L^1 = \frac{h}{c}$. Thus, (2) leads to $\tau_1^{\mathrm{MTP}}(x_L) = \frac{h}{c}$ and $\tau_1^{\mathrm{MTP}}(x_\ell) = 0$ for all $\ell \in \mathcal{N}_L$, and then $\tau_1^{\mathrm{MTP}}(x_R) = 0$. Now, we consider the induction step. Thus, assuming that (6a) and (6b) hold, we use (2) to write $\tau_{2n+2}^{\mathrm{MTP}}(x_\ell) = \tau_{2n+1}^{\mathrm{MTP}}(x_\ell) + v_R^{2n+2}\phi_R(x_\ell)$ for $\ell \in \{R, L\}$. Using (5) with the fact that the decomposition is uniform, we obtain for $\ell \in \mathcal{N}_R$ that

$$v_R^{2n+2} = \frac{h}{c} + \tau_{2n+1}^{\mathrm{MTP}}(x_\ell) - \tau_{2n+1}^{\mathrm{MTP}}(x_R) = \frac{h}{c} + (2n+1)\frac{h}{c} - 2n\frac{h}{c} = 2\frac{h}{c},$$

and thus $\tau_{2n+2}^{\mathrm{MTP}}(x_L) = (2n+1)\frac{h}{c}$ and $\tau_{2n+2}^{\mathrm{MTP}}(x_R) = (2n+2)\frac{h}{c}$. Now, (2) implies that $\tau_{2n+3}^{\mathrm{MTP}}(x_\ell) = \tau_{2n+2}^{\mathrm{MTP}}(x_\ell) + v_L^{2n+2}\phi_L(x_\ell)$ for $\ell \in \{R, L\}$, and (5) allows us to compute $v_L^{2n+2} = 2\frac{h}{c}$. Hence, we get that $\tau_{2n+3}^{\mathrm{MTP}}(x_L) = (2n+3)\frac{h}{c}$ and $\tau_{2n+3}^{\mathrm{MTP}}(x_R) = (2n+2)\frac{h}{c}$, and the claim follows. $\qquad\square$

3 Red-black Schwarz waveform relaxation (RBSWR)

Consider a decomposition of Ω into $N-1$ subdomains $I_j = (x_j, x_{j+2})$, $j = 0, \dots, N-2$, where x_j are the nodes in Ω_0. This is a decomposition with generous overlap. Let $\mathcal{R} = \{0, 2, 4, \dots\}$ and $\mathcal{B} = \{1, 3, 5, \dots\}$ be two subsets of $\{0, 1, \dots, N-2\}$. RBSWR is defined by solving in parallel the subproblems

$$\partial_{tt} u_j^k(x,t) = c^2 \partial_{xx} u_j^k(x,t) \qquad\qquad \text{in } I_j \times (0,T), \qquad (7)$$

$$u_j^k(x,0) = g_0(x) \text{ and } \partial_t u_j^k(x,0) = g_1(x) \qquad \text{for } x \in I_j, \qquad (8)$$

$$u_j^k(x_j,t) = u_{j-1}^{k-1}(x_j,t) \qquad\qquad \text{for } t \in [0,T], \qquad (9)$$

$$u_j^k(x_{j+2},t) = u_{j+1}^{k-1}(x_{j+2},t) \qquad\qquad \text{for } t \in [0,T], \qquad (10)$$

where k is the iteration index, and $j \in \mathcal{R}$ for k odd and $j \in \mathcal{B}$ for k even. Moreover, the exterior boundary conditions have to be appropriately replaced for $j = 0$ at x_0 and for $j = N-2$ at x_{N-1}. Now, we assume that the decomposition Ω_0 is uniform and denote the overlap by $\delta = x_j - x_{j-1}$. Convergence of (7) was proved in [3, Theorem 1], where it is shown that the exact solution is obtained for $k \geq \frac{Tc}{\delta}$. The convergence behavior depends on the propagation of the exact solution in the overlap; see [3, Figure 1] and Fig. 1, bottom right. In particular, it is possible to show that at odd iterations $k = 2n+1$, $n = 0, 1, 2, \dots$, the exact solution is computed in the overlap below the characteristic curve intersecting the interface $\{x_L\} \times (0,T)$ at $(2n+1)\frac{\delta}{c}$, cf. Fig. . 1, bottom right. Similarly, at even iterations $k = 2n$, $n = 1, 2, \dots$, the exact
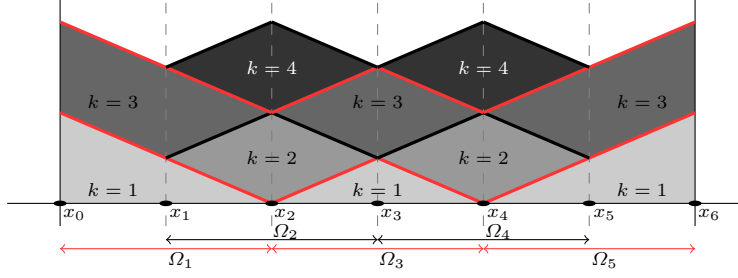
Fig. 2 First four iterations of the red-black SWR for a 5-subdomain case. The gray areas are the regions where the exact solution is computed.

solution is computed in the overlap below the characteristic curve intersecting the interface $\{x_R\} \times (0, T)$ at $2n\frac{\delta}{c}$, cf. Fig. . 1, bottom right. Thus, we can define a *RBSWR advancing front*, denoted by $\tau_k^{\text{RBSWR}}(x)$, as the function lying on the characteristic curves and such that below its graph the method has already computed the exact solution, independently of the initial guess u^0. An example of the first 4 iterations of RBSWR is given in Fig. 2. The fronts $\tau_k^{\text{RBSWR}}(x)$ are red and black lines delimiting the gray regions where the exact solution has been computed.

The RBSWR advancing front is characterized in the next lemma, whose proof can be deduced from Fig. 1, bottom right, and Fig. 2.

Lemma 2 (RBSWR advancing front)

Assume that the decomposition Ω_0 is uniform with $h = x_j - x_{j-1}$ for $j = 1, \ldots, N$. Consider any interior subinterval $\mathcal{I} = [x_L, x_R]$, with $R \in \mathbb{N}$ even and $L = R - 1$. Consider the RBSWR with overlap $\delta = x_R - x_L$ and initialized with any (sufficiently regular) function u^0 such that $\tau_0^{\text{RBSWR}} \equiv 0$. The advancing front τ_k^{RBSWR} satisfies $\tau_1^{\text{RBSWR}}(x_L) = \frac{\delta}{c}$, $\tau_1^{\text{RBSWR}}(x_R) = 0$, and, for any $n = 1, 2, \ldots$, the relations

$$\tau_{2n}^{\text{RBSWR}}(x_L) = (2n-1)\delta/c, \qquad \tau_{2n}^{\text{RBSWR}}(x_R) = 2n\delta/c, \qquad (11a)$$

$$\tau_{2n+1}^{\text{RBSWR}}(x_L) = (2n+1)\delta/c, \qquad \tau_{2n+1}^{\text{RBSWR}}(x_R) = 2n\delta/c. \qquad (11b)$$

The relation between MTP and RBSWR arises immediately by comparing Lemma 1 and Lemma 2 and it is stated in the following theorem.

Theorem 1 (RBSWR and MPT for uniform decompositions)

Consider a uniform decomposition Ω_0 with $h = x_j - x_{j-1}$ for $j = 1, \ldots, N$. Assume that the (parallel) MTP selects alternately odd and even nodes of Ω_0 at odd and even iterates, respectively. Further, notice that the overlap is $\delta = h$. Then, for any initial guess u^0 such that $\tau_0^{\text{RBSWR}} \equiv 0$, the fronts τ_k^{MTP} and τ_k^{RBSWR} coincide in all interior nodes of Ω_0, thus in all interior subintervals.
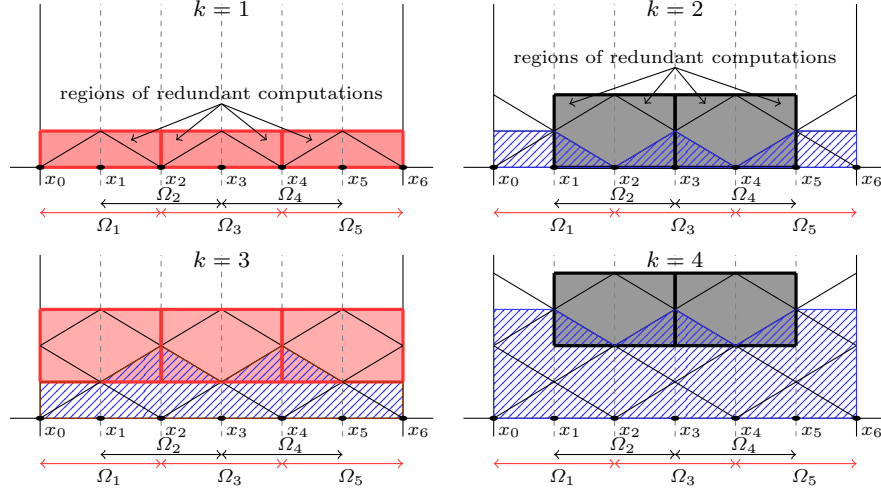
Fig. 3 First four iterations of UTP on a 5 subdomain decomposition. Red and black boxes are the space-time subdomains constructed by UTP at odd and even iterations. The black lines correspond to the tents that MTP constructs. The blue hatched regions are the portions of the domain where UTP computes the exact solution.

4 Unmapped tent-pitching

Theorem 1 suggests that the mapping process is not necessary to obtain the exact solution below the tents. This process can be avoided by using SWR on appropriately defined space-time subdomains, even though few redundant computations need to be performed. The key idea is to consider rectangular space-time subdomains having the same height of the tents pitched on the space subdomains and width equal to the length of the space subdomains themselves. The space-time subdomains can be considered as rectangular tents, in which the solution can be computed directly, using, e.g., a time-stepping method, without the need of mapping the tent into a rectangular box (the subdomain is already a rectangular tent!). We call this approach the *unmapped tent pitching* (UTP) algorithm, and describe it in detail for a uniform space decomposition Ω_0 and for a parallel MTP selecting alternatingly odd and even nodes. Extensions to nonuniform decompositions and higher dimensions are possible, but beyond the scope of this short manuscript. They will be presented in the future work [1]. The UTP process begins by selecting the odd nodes of Ω_0 and computing the heights v_j^0 of the tents that the MTP would pitch. Instead, rectangular space-time subdomains $\mathcal{T}_j$ are pitched, and one RBSWR iteration is performed restricted on them. This step is shown in Fig. 3, top left, where the three (red) subdomains are represented together with the tents that the parallel MTP would pitch. RBSWR computes the exact solution below the tents, as represented by the blue hatched regions in

---

Algorithm 2 Unmapped Tent Pitching by RBSWR

Require: A decomposition Ω_0 of N nodes and an initial guess function u^0.
 1: Set $k = 1$ and $v_j^0 = 0$ for all $j = 1, \ldots, N$.
 2: **while** $\exists j \in \{0, 1, \ldots, N-1\} \, : \, v_j^{k-1} \neq T$ **do**
 3:     Set $J_k = \{1, 3, \ldots\}$ if k is odd and $J_k = \{2, 4, \ldots\}$ if k is even.
 4:     Use (5) to compute the heights $v_j^k = w_j^k + v_j^{k-1}$ for all $j \in J_k$.
 5:     For each $j \in J_k$ pitch a rectangular subdomain $\mathcal{T}_j := [x_{j-1}, x_{j+1}] \times [v_j^{k-1}, v_j^k]$.
 6:     Solve (7) to get u_j^{k+1} in $\mathcal{T}_j$ for all $j \in J_k$, and extend them by u^0 above $\mathcal{T}_j$.
 7:     Update $k = k + 1$.
 8: **end while**

Fig. 3, top right. However, wrong approximations are computed in the areas above the tents, which correspond to the regions where redundant computations are performed. The second iteration of the UTP is shown in Fig. 3, top right. Here, the new pitched rectangular subdomains are depicted in black. Within them one RBSWR iteration is performed. The exact solution is obtained below the classical MTP tents, while redundant computations are performed above them. As a result, the exact solution is computed in the blue hatched area depicted in Fig. 3, bottom left. By repeating this process iteratively one obtains the subdomains and the exact solution areas shown in Fig. 3 for $k = 3$ and $k = 4$. The overall UTP Algorithm 2 terminates when the exact solution is computed in the entire space-time domain.

To conclude, our new unmapped tent pitching algorithm computes to the mapped tent pitching algorithm equivalent approximations, using redundant computations. It is however cheaper, since it does not have to compute the tent mappings, and the volume of the redundant computations is also present in the tents after the mapping. Its implementation is also straightforward, and one can use standard time integrators, since there is no danger of order reduction without the tent mapping.

References

1. G. Ciaramella, M.J. Gander, and I. Mazzieri. Space-time RAS methods for wave-propagation problems. *in preparation*, 2023.
2. R. Courant, K. Friedrichs, and H. Lewy. On the partial difference equations of mathematical physics. *IBM J. Res. Dev.*, 11(2):215–234, 1967.
3. M. J. Gander, L. Halpern, and F. Nataf. Optimal convergence for overlapping and non-overlapping Schwarz waveform relaxation. *Proceedings in Domain Decomposition Methods in Science and Engineering XIX*, 1999.
4. J. Gopalakrishnan, J. Schöberl, and C. Wintersteiger. Mapped tent pitching schemes for hyperbolic systems. *SIAM J. Sci. Comput.*, 39(6):B1043–B1063, 2017.
5. J. Nievergelt. Parallel methods for integrating ordinary differential equations. *Commun. ACM*, 7(12):731–733, 1964.

MOX Technical Reports, last issues

Dipartimento di Matematica
Politecnico di Milano, Via Bonardi 9 - 20133 Milano (Italy)

81/2022   Bonizzoni, F.; Hauck, M.; Peterseim, D.
A reduced basis super-localized orthogonal decomposition for reaction-convection-diffusion problems

82/2022   Ciaramella, G.; Gander, M.; Van Criekingen, S.; Vanzan, T.
A PETSc Parallel Implementation of Substructured One- and Two-level Schwarz Methods

80/2022   Balduzzi, G.; Bonizzoni, F.; Tamellini, L.
Uncertainty quantification in timber-like beams using sparse grids: theory and examples with off-the-shelf software utilization

78/2022   Bucelli, M.; Gabriel, M. G.; Gigante, G.; Quarteroni, A.; Vergara, C.
A stable loosely-coupled scheme for cardiac electro-fluid-structure interaction

79/2022   Antonietti, P. F.; Farenga, N.; Manuzzi, E.; Martinelli, G.; Saverio, L.
Agglomeration of Polygonal Grids using Graph Neural Networks with applications to Multigrid solvers

77/2022   Ziarelli, G.; Dede', L.; Parolini, N.; Verani, M.; Quarteroni, A.
Optimized numerical solutions of SIRDVW multiage model controlling SARS-CoV-2 vaccine roll out: an application to the Italian scenario.

76/2022   Spreafico, M.; Ieva, F.; Fiocco, M.
Longitudinal Latent Overall Toxicity (LOTox) profiles in osteosarcoma: a new taxonomy based on latent Markov models

73/2022   Spreafico, M.; Gasperoni, F.; Barbati, G.; Ieva, F.; Scagnetto, A.; Zanier, L.; Iorio, A.; Sinagra, G.; Di Lenarda, A.
Adherence to disease-modifying therapy in patients hospitalized for HF: findings from a community-based study

70/2022   Andrini, D.; Balbi, V.; Bevilacqua, G.; Lucci, G.; Pozzi, G.; Riccobelli, D.
Mathematical modelling of axonal cortex contractility

71/2022   Calabrò, D.; Lupo Pasini, M.; Ferro, N.; Perotto, S.
A deep learning approach for detection and localization of leaf anomalies